THE
EMBO
JOURNAL

PACAP type I receptor transactivation is essential for IGF-1 receptor signalling and antiapoptotic activity in neurons

Nicolas Delcourt[1,2,3,4,5], Eric Thouvenot[1,2,3,4,5], Benjamin Chanrion[1,2,3,4,5], Nathalie Galéotti[1,2,3,4,5], Patrick Jouin[1,2,3,4,5], Joël Bockaert[1,2,3,4,5,]* and Philippe Marin[1,2,3,4,5]

[1]CNRS UMR 5203, Montpellier, France, [2]INSERM, U661, Montpellier, France, [3]University Montpellier I, Montpellier, France, [4]University Montpellier II, Montpellier, France and [5]Département de Neurobiologie, Institut de Génomique Fonctionnelle, Montpellier, France

Insulin-like growth factor-1 (IGF-1) and pituitary adenylyl cyclase activating polypeptide (PACAP) are both potent neurotrophic and antiapoptotic factors, which exert their effects via phosphorylation cascades initiated by tyrosine kinase and G-protein-coupled receptors, respectively. Here, we have adapted a recently described phosphoproteomic approach to neuronal cultures to characterize the phosphoproteomes generated by these neurotrophic factors. Unexpectedly, IGF-1 and PACAP increased the phosphorylation state of a common set of proteins in neurons. Using PACAP type 1 receptor (PAC1R) null mice, we showed that IGF-1 transactivated PAC1Rs constitutively associated with IGF-1 receptors. This effect was mediated by Src family kinases, which induced PAC1R phosphorylation on tyrosine residues. PAC1R transactivation was responsible for a large fraction of the IGF-1-associated phosphoproteome and played a critical role in the antiapoptotic activity of IGF-1. Hence, in contrast to the general opinion that the trophic activity of IGF-1 is solely mediated by tyrosine kinase receptor-associated signalling, we show that it involves a more complex signalling network dependent on the PAC1 Gs-protein-coupled receptor in neurons.

Introduction

Among polypeptide neurotrophic factors that participate in neuronal differentiation during CNS development, insulin-like growth factor-1 (IGF-1) is of particular interest. IGF-1 is the growth factor that initiates axon specification and, thus, plays an essential role in the establishment of neuronal

*Corresponding author. Département de Neurobiologie, Institut de Génomique Fonctionnelle, 141 Rue de la Cardonille, 34094 Montpellier Cedex 5, France. Tel.: +33 467 14 29 30; Fax: +33 467 14 29 10; E-mail: joel.bockaert@igf.cnrs.fr

polarity (Sosa *et al*, 2006). IGF-1 is also highly expressed in the mature nervous system and has been shown to exert neuroprotective effects upon numerous neuronal populations (D'Mello *et al*, 1993; Galli *et al*, 1995; Kaspar *et al*, 2003; Leinninger *et al*, 2004; Vincent *et al*, 2004). IGF-1 is a potent agent for rescuing neurons from apoptosis and the ability of IGF-1 to promote neuronal survival is associated with its ability to prevent apoptosis. Similarly, pituitary adenylyl cyclase activating polypeptide (PACAP) is a unique polypeptide neurotransmitter capable of providing neuroprotective or neurotrophic action upon various neuronal populations throughout the CNS (Arimura *et al*, 1994; Morio *et al*, 1996; Villalba *et al*, 1997; Takei *et al*, 1998, 2000). PACAP also exerts chemotropic effects on developing growth cones (Guirland *et al*, 2003) and plays a crucial role in the control of cerebral cortical progenitor division (Suh *et al*, 2001; Carey *et al*, 2002).

Neurotrophic activities of both IGF-1 and PACAP are initiated by specific kinase-dependent signalling cascades. IGF-1 triggers autophosphorylation of its cognate tyrosine kinase receptor on multiple tyrosines. These phosphotyrosine residues serve as platforms for the binding and subsequent phosphorylation of various signalling molecules, thus initiating multiple signalling cascades. For instance, the phosphatidyl inositol 3-kinase (PI3-K)/Cdc42 pathway is essential for the determination of neuronal polarity (Sosa *et al*, 2006), whereas the PI3-K/Akt pathway mediates the IGF-1 antiapoptotic activity (Datta *et al*, 1997; Dudek *et al*, 1997). In contrast, PACAP has been shown to protect neurons against apoptosis via a signalling pathway involving Gs-protein-coupled PAC1 receptor, protein kinase A (PKA) and mitogen-activated protein kinase (Erk1,2) (Villalba *et al*, 1997; Vaudry *et al*, 1999). Similarly, the chemotropic effects of PACAP on developing growth cones are mediated by the cAMP/PKA signalling pathway (Guirland *et al*, 2003). In contrast, the nature of downstream effector proteins that are phosphorylated upon activation of each of these signalling cascades remains largely unexplored.

Results and discussion

Efficient enrichment of phosphoproteins from IGF-1- or PACAP-treated cortical neurons afforded by metal-affinity chromatography

To get an unbiased overview of the IGF-1 and PACAP receptor-associated phosphoproteomes in cortical neurons, we used a phosphoproteomic approach that we adapted for the first time to neuronal cultures containing only 10 million neurons. This approach was based on phosphoprotein enrichment by metal-affinity chromatography (PMAC), followed by the separation of affinity-purified proteins onto two-dimensional (2D) gels and their identification by MALDI-TOF mass spectrometry (MS). Phosphopeptides
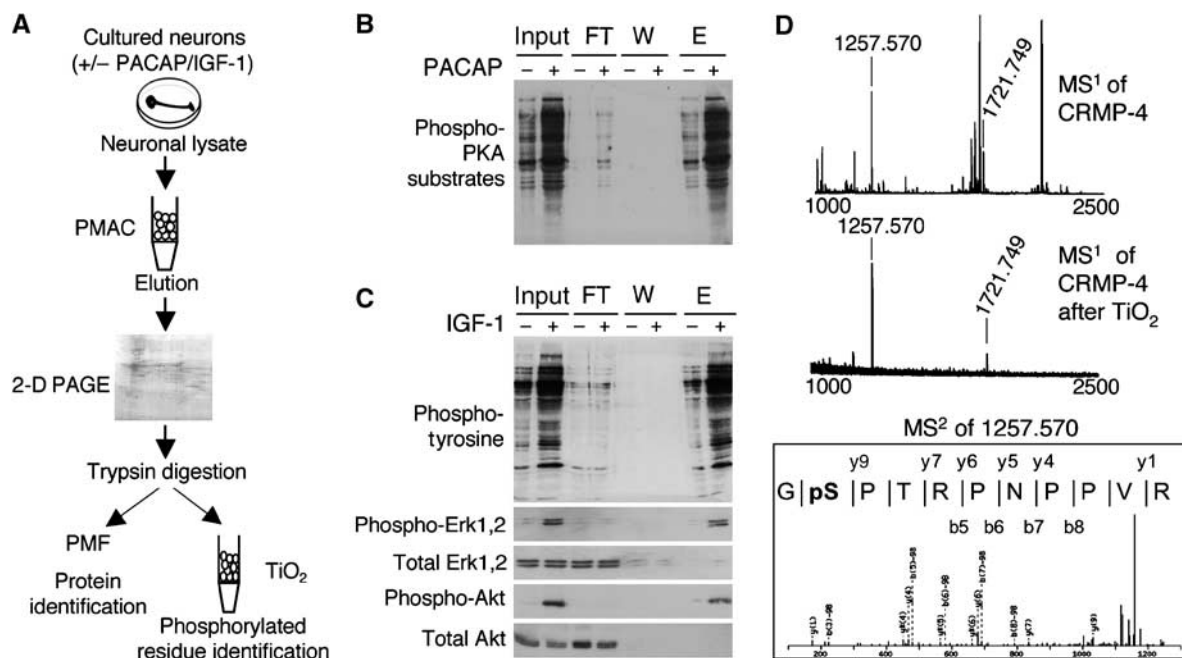
Figure 1 Principle and validation of the phosphoproteomic approach. (**A**) Strategy used for the enrichment and identification of phospho-proteins in cortical neurons. Mice cortical neurons grown for 7 days in serum-free medium were exposed for 10 min to either IGF-1 (2.5 ng/ml) or PACAP (1 nM). Neurons were lysed and protein extracts were enriched in PMAC. The phosphoprotein-enriched fraction was then separated onto 2D gels. Proteins were digested by trypsin and identified by MALDI-TOF-MS-based peptide mass fingerprinting (PMF). Protein-derived tryptic phosphopeptides were purified in parallel using TiO_2 microcolumns and analyzed by MALDI-MS/MS to identify phosphorylated residues. (**B, C**) Efficiency of PMAC to retain phosphoproteins. Total neuronal protein extracts (input), and various fractions (flow through (FT), washing medium (W) and eluate (E)) obtained by PMAC were analyzed by Western blotting using antibodies against phospho-PKA substrates (B), phospho-tyrosine, phospho-Erk1,2 and phospho-Akt and antibodies recognizing Erk1,2 and Akt independently of their phosphorylation state (C). (**D**) MS analysis of CRMP-4 tryptic digest before (top) and after (bottom) phosphopeptide purification on TiO_2 microcolumns. The identification of the phosphorylated residue in the 1257.570 Da peptide (corresponding to phospho-Ser[522] in the CRMP4 sequence) was performed by MALDI-MS/MS.

resulting from trypsin digestion of phosphoproteins were also purified on titanium dioxide (TiO_2) microcolumns to identify phosphorylated residues by MS/MS (Figure 1A; Collins *et al*, 2005; Larsen *et al*, 2005). We first evaluated the efficiency of the PMAC procedure for enrichment of phosphorylated proteins by immunoblotting using various phosphoprotein-specific antibodies. As illustrated in Figure 1B, treating cortical neurons for 10 min with PACAP (1 nM) resulted in the phosphorylation of PKA substrates. Most of phosphorylated PKA substrates were retained on the PMAC column. Similarly, most of proteins phosphorylated on tyrosine residues upon IGF-1 treatment (10 min, 2.5 ng/ml) bound to PMAC beads (Figure 1C). Finally, analysis of specific signalling proteins such as Erk1,2 and Akt revealed that IGF-1- (Figure 1C) or PACAP- (not shown) generated phospho-Erk1,2 and phospho-Akt were entirely retained on the PMAC column. These experiments also indicated that a minor fraction of total Erk1,2 and Akt was retained on PMAC beads (and then eluted with phosphate buffer), underpinning the low phosphorylation stoichiometry of several molecules involved in signalling cascades initiated by these neurotrophic factors in neurons.

Phosphorylation of a common set of proteins in IGF-1- or PACAP-treated neurons

2D gel analysis of PMAC-purified proteins from neurons challenged with either IGF-1 or PACAP revealed that both treatments induced a large increase in the amount of proteins retained by PMAC beads (Figure 2A, upper gels). To assess

possible binding of non-phosphorylated proteins on PMAC beads together with the phosphorylated ones, we performed metabolic labelling of neurons with ^{32}P-orthophosphate before the PMAC procedure and separated radioactively labelled proteins onto 2D gels. These experiments confirmed that IGF-1 and PACAP induced a large increase in the phosphorylation state of a set of neuronal proteins (Figure 2A, lower gels). Further supporting efficient binding of phosphoproteins to the PMAC beads, we detected only traces of radioactive proteins in the PMAC flow-through fraction (Supplementary Figure S1). However, comparing silver-stained and ^{32}P-labelled 2D protein patterns in the PMAC-purified fraction revealed some differences. Indeed, a number of proteins retained on PMAC beads were not labelled with [32]P (Figure 2A). Therefore, only ^{32}P-labelled proteins that were retained on PMAC beads were further analyzed. Seventy spots (or trains of spots) fulfilling this criterion were identified by MALDI-TOF-MS-based peptide mass fingerprinting. These spots corresponded to 51 different proteins, which were assigned to eight major protein categories with regard to their biological function (Figure 2B). These include nuclear proteins, signalling or adhesion molecules, cytoskeleton proteins, chaperone proteins, translation factors or proteins controlling translation, metabolic enzymes, proteasome subunits and proteins involved in the regulation of axonal growth (Figure 2B; see also Supplementary Table S1).

Surprisingly, more than 80% of the identified phospho-proteins were phosphorylated following exposure of neurons to both IGF-1 and PACAP (Figure 2C), which, however, are
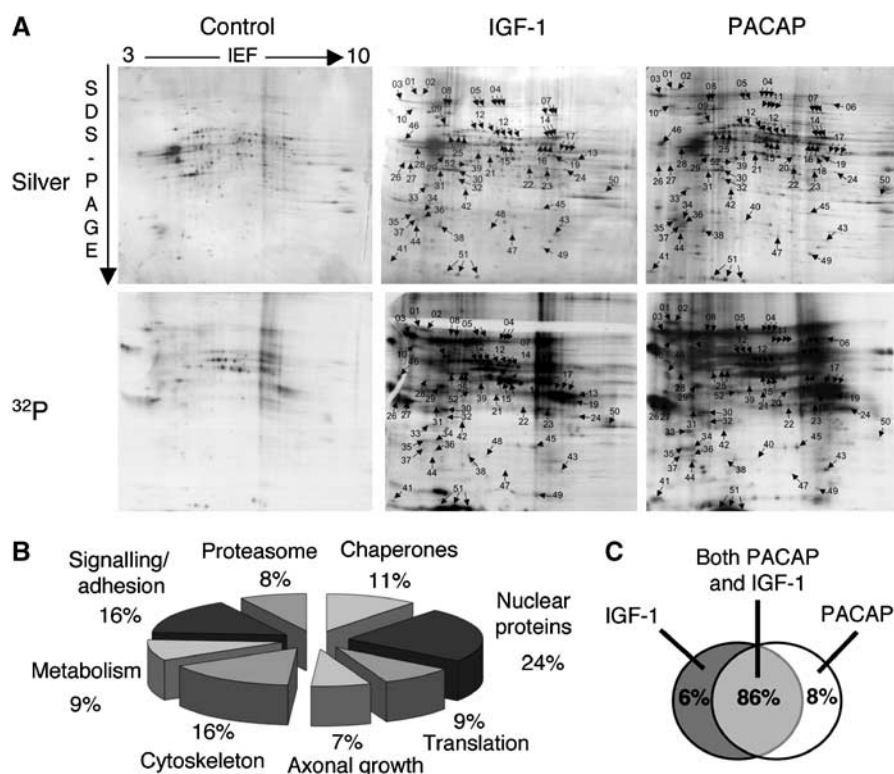
Figure 2 Phosphorylation of a common set of proteins in cortical neurons exposed to IGF-1 and PACAP. (**A**) Cortical neurons grown for 7 days in 100-mm culture dishes ($\sim 10^7$ neurons) were incubated for 3 h in phosphate-free HEPES buffer in the absence (top gels) or presence of ^{32}P-orthophosphoric acid (bottom gels, 5 mCi/dish) before they were exposed or not to either IGF-1 (2.5 ng/ml) or PACAP (1 nM) for 10 min. PMAC phosphoprotein-enriched fractions were separated onto 2D gels and proteins were revealed either by silver staining or autoradiography. Matching between silver-stained and ^{32}P-labelled spots was performed using the Melanie 5 software (GE Healthcare). Arrows represent phosphoproteins that were identified by PMF. Spot numbers refer to the proteins listed in Supplementary Table S1. Representative gels out of the four gels obtained from different cultures for each experimental condition are illustrated. (**B**) Pie chart representation of the phosphoprotein categories identified in cortical neurons treated with IGF-1 or PACAP. (**C**) Schematic representation of the common protein phosphorylation pattern in cortical neurons in response to IGF-1 and PACAP treatments (proteins indexed in A and listed in Supplementary Table S1).

known to initiate distinct signalling cascades. We thus sought to identify phosphorylated residues in a subset of proteins phosphorylated in response to both IGF-1 and PACAP treatments, using a procedure based on the enrichment of phosphopeptides resulting from trypsin digestion of these phosphoproteins on TiO$_2$ microcolumns. We first validated the selectivity for phosphopeptides of the TiO$_2$ beads on tryptic peptides originating from collapsin response mediator protein-4 (CRMP-4, spot 15; Supplementary Table S1 and Figure 2A), a protein known to be phosphorylated on several serine and threonine residues. MALDI-TOF-MS spectra of the tryptic digest of CRMP-4 without TiO$_2$ enrichment and after TiO$_2$ chromatography indicated that only a few peptides were eluted off the TiO$_2$ column, compared with the unpurified peptide mixture (Figure 1D). The most intense signals corresponded to two peptides of molecular masses of 1257.570 and 1721.749 Da. These peptides were shown to be phosphorylated on Ser^{522} (Figure 1D) and Thr^{509} residues, respectively, following exposure of neurons to either IGF-1 or PACAP, as assessed by MALDI-MS/MS (Supplementary Table S2). These results highlight the remarkable selectivity of TiO$_2$ chromatography toward phosphorylated peptides within a complex peptide mixture containing a minority of phosphopeptides. Both IGF-1 and PACAP also increased the phosphorylation of the Ser^{522} and Thr^{509} residues of CRMP-2 as well as the Ser^{522} of CRMP1. Similarly, stathmin was found to be phosphory-

lated on Ser^{24} residue in both IGF-1- and PACAP-treated neurons (Supplementary Table S2).

Altogether, these findings indicate that IGF-1 and PACAP induce similar phosphorylation profiles in cortical neurons, even though they are known to activate distinct signalling cascades. In contrast, selective activation of group I metabotropic glutamate receptor by (*S*)-3,5-dihydroxyphenylglycine (DHPG), which like IGF-1 and PACAP is known to prevent neuronal apoptosis (Copani *et al*, 1998), induced the phosphorylation of a distinct protein pattern in neurons (Supplementary Figure S2). Overall, DHPG was less potent than IGF-1 or PACAP to induce phosphorylation of neuronal proteins. Only 18 out of the 51 proteins phosphorylated upon PACAP or IGF-1 treatments were phosphorylated in neurons following a DHPG exposure, which induced the phosphorylation of three additional proteins that were not identified in the PACAP- or IGF-1-associated phosphoproteomes. This indicates that various treatments supporting neuronal survival do not trigger phosphorylation of a unique set of neuronal proteins.

Transactivation of epidermal growth factor receptor in neurons exposed to IGF-1 or PACAP
We hypothesized that the common phosphorylation pattern detected in neurons exposed to PACAP or IGF-1 could result from the transactivation of a tyrosine kinase receptor follow-

ing PACAP exposure. Indeed, PACAP was found previously to increase TrkA tyrosine kinase activity in PC12 cells and to activate TrkB in hippocampal neurons (Lee et al, 2002; Rajagopal et al, 2004). However, these transactivation processes required a longer PACAP exposure (3 h), compared with those performed in our study (10 min). Alternatively, ligands of Gs-coupled receptors can induce a rapid transactivation of the epidermal growth factor receptor (EGFR) through a signalling cascade involving cAMP and PKA (Bertelsen et al, 2004). Consistently, we showed that PACAP, as IGF-1, stimulated the phosphorylation of the EGFR on Tyr^{845} and on Tyr^{1068} residues (Supplementary Figure S3A). Tyrosine phosphorylation of the EGFR induced by PACAP was strongly decreased by Rp-cAMPS (10 μM), an inhibitor of PKA, but was unchanged in the presence of U73122, a phospholipase Cβ inhibitor, indicating that transactivation of EGFR in neurons exposed to PACAP was dependent on PKA activation (Supplementary Figure S3A). Because autophosphorylation of the EGFR on Tyr^{1068} is known to be involved in the activation of the mitogen-activated protein kinase Erk1,2 pathway, we examined whether EGFR transactivation was involved in the increase in Erk1,2 phosphorylation measured in neurons exposed to PACAP. As shown in Supplementary Figure S3B, AG1478 (250 nM), a specific inhibitor of EGFR kinase activity, strongly decreased the phosphorylation of Erk1,2 induced by PACAP. Rp-cAMPS also strongly attenuated the phosphorylation of Erk1,2 induced by PACAP, consistent with the role of PKA in EGFR transactivation. We next examined whether EGFR transactivation contributed to the common phosphorylation events detected in neurons challenged with IGF-1 or PACAP. Blocking EGFR activity with AG1478 only suppressed the phosphorylation of three out of 48 proteins that were phosphorylated upon PACAP treatment and purified on PMAC beads (Supplementary Figure S3C). Moreover, AG1478 treatment did not alter protein phosphorylation in neurons exposed to IGF-1 (not shown). Taken together, these results indicate that EGFR transactivation only plays a minor role in generating the common IGF-1 and PACAP-associated phosphoproteomes in cortical neurons.

Transactivation of PAC1 receptor in neurons exposed to IGF-1

We next examined the possibility that IGF-1R was transactivated upon PACAP treatment. As illustrated in Figure 3A, IGF-1, but not PACAP, increased the phosphorylation of the IGF-1R on Tyr$^{1135/1136}$, two residues that are known to be involved in the activation of the IGF-1R. This indicates that PACAP treatment does not activate IGF-1R in neurons. Because recent studies demonstrated that first, IGF-1 could transactivate two GPCRs, the chemokine receptor CXCR4 and the sphingosine 1-phosphate (S1P) receptor (Akekawatchai et al, 2005; El-Shewy et al, 2006) and, second, that IGF-1R stimulation could activate PKA in neurons (Subramaniam et al, 2005), we hypothesized that IGF-1 could transactivate PACAP type 1 receptor (PAC1R) in neurons. We first confirmed that treating cortical neurons with IGF-1 increased the phosphorylation level of PKA substrates and that this effect was blocked by Rp-cAMPS (Figure 3B). Next, using cultured cortical neurons from PAC1R null (PAC1$^{-/-}$) mice (Jamen et al, 2000), we demonstrated that the phosphorylation of PKA substrates induced by IGF-1 was dependent on the

expression of functional PAC1Rs (Figure 3B). Consistent with this finding, IGF-1 increased intracellular cAMP level in neurons from wild-type (WT) mice but not PAC1$^{-/-}$ mice (Figure 3C). The lack of cAMP production and phosphorylation of PKA substrates in mutant mice neurons exposed to IGF-1 did not result from a decrease in IGF-1R expression or responsiveness. Indeed, IGF-1 increased to a similar extent IGF-1R phosphorylation on Tyr$^{1135/1136}$ residues in neurons from WT and PAC1$^{-/-}$ mice, which expressed identical IGF-1R levels (Supplementary Figure S4). Moreover, PAC1Rs were not activated secondary to the release of PACAP from neurons exposed to IGF-1. Accordingly, blocking PAC1R by PACAP6-38 (10 nM), a competitive antagonist that suppressed PACAP-induced phosphorylation of PKA targets (not shown), did not prevent the IGF-1-evoked increase in the phosphorylation state of PKA substrates (Figure 3B), indicating that IGF-1 transactivated unliganded PAC1R. This contrasts with the IGF-1-mediated transactivation of S1PR, which resulted from increased S1P synthesis and accumulation of extracellular S1P (El-Shewy et al, 2006).

NGF treatment (100 nM) elevated cAMP levels in cortical neurons (Figure 3C), consistent with previous findings (Stessin et al, 2006). However, contrasting with the IGF-1 effect, NGF increased cAMP level to a similar extent in neurons from WT and PAC1$^{-/-}$ mice. This indicates that PAC1R could not be transactivated by any tyrosine kinase receptor ligand except IGF-1, underpinning the specificity of the crosstalk between IGF-1 and PAC1 receptors. Finally, we examined whether PAC1R transactivation contributed to the IGF-1R-associated phosphoproteome. We showed that the increased phosphorylation of 20 out of 48 proteins induced by IGF-1 treatment was suppressed in neurons from PAC1$^{-/-}$ mice (Figure 3D). These include proteins involved in neuronal growth and migration such as drebrin (Hayashi and Shirao, 1999), doublecortin (Bai et al, 2003; Tanaka et al, 2004) or GAP-43 (Aigner et al, 1995) and proteins potentially involved in the control of apoptosis, such as translation elongation factor-2 (Marin et al, 1997), the heterogeneous ribonucleoprotein hnRNP-D0 (Lapucci et al, 2002), the phosphatase inhibitor SET (Fan et al, 2003) and 14-3-3 proteins (Datta et al, 2000). Consistent with a critical role of PAC1R transactivation in IGF-1R-associated phosphoproteome, the IGF-1-evoked increase in the phosphorylation of Akt at Ser^{473} (a process involved in Akt activation by the PI3-K pathway) was markedly reduced in PAC1$^{-/-}$ neurons, compared with that measured in WT neurons (Figure 3E). This result demonstrates a role of PAC1R transactivation in the initial steps of the signalling cascade initiated by IGF-1R activation.

Role of Src family kinases in IGF-1-mediated PAC1 receptor transactivation

IGF-1 did not alter [^{125}I]PACAP27 binding at PAC1R (Supplementary Figure S5), indicating that IGF-1-induced PAC1R transactivation did not result from its binding to the PACAP-binding site on PAC1Rs. Co-immunoprecipitation experiments performed on lysates from cortical neurons transfected with a vesicular stomatitis virus glycoprotein epitope-tagged mouse PAC1R (VSV-PAC1R) using an anti-VSV antibody revealed that PAC1Rs constitutively associated with IGF-1Rs (Figure 4A). We next examined the possibility that PAC1R transactivation occurred via stimulation of a kinase that regulates PAC1 receptor activity, using inhibitors
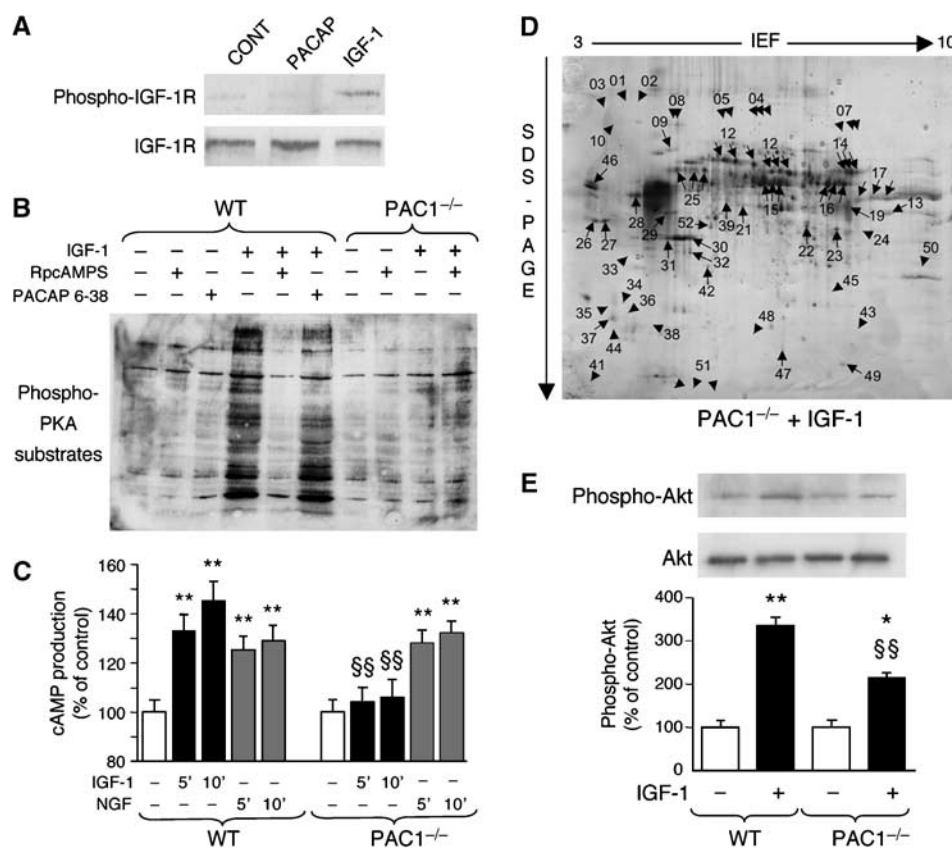
Figure 3 Transactivation of PAC1 receptor by IGF-1 in cortical neurons. (**A**) PACAP does not transactivate the IGF-1R. Cortical neurons were exposed for 10 min to PACAP (1 nM) or IGF-1 (2.5 ng/ml). IGF-1R activation was assessed by sequential immunoblotting with an antibody against IGF-1Rs phosphorylated on $Tyr^{1135/1136}$ and an antibody recognizing the IGF-1R independently of its phosphorylation state. (**B**) IGF-1-induced PKA activation is mediated by the PAC1R. Cortical neurons from WT or $PAC1^{-/-}$ mice were exposed for 10 min to IGF-1 in the absence or presence of either Rp-cAMPS (10 µM) or PACAP6-38 (10 nM). PKA activation was assessed by Western blotting using an antibody against phospho-PKA substrates. (**C**) IGF-1 but not NGF induces cAMP production in a PAC1R-dependent manner. Cortical neurons from WT or $PAC1^{-/-}$ mice were exposed to IGF-1 or NGF (100 nM) for 5 or 10 min in the presence of 1 mM IBMX and intracellular cAMP content was quantified using an HTRF-based kit. Results, expressed in % of basal cAMP level, are means±s.e.m. of values obtained in five independent experiments. **$P<0.01$, versus corresponding values measured in untreated neurons; §§$P<0.01$, versus corresponding values measured in WT neurons (ANOVA followed by the Student–Newman–Keul test). (**D**) IGF-1R-associated phosphoproteome in $PAC1^{-/-}$ neurons. Cortical neurons from $PAC1^{-/-}$ mice were treated with IGF-1 (2.5 ng/ml) for 10 min and proteins purified by PMAC were separated on 2D gels and stained with silver. The arrowheads indicate the position of spots whose phosphorylation in response to IGF-1 treatment is inhibited in neurons from $PAC1^{-/-}$ mice. (**E**) PAC1R transactivation contributes to the phosphorylation of Akt induced by IGF-1 in cortical neurons. Cultured cortical neurons from WT and $PAC1^{-/-}$ mice were treated for 10 min with IGF-1 (2.5 ng/ml) and the phosphorylation of Akt was analyzed by sequential immunoblotting with antibodies against phospho-Ser^{473}Akt and total Akt. Quantification of Akt phosphorylation was performed by densitometric analysis using the NIH Image software. Data are means±s.e.m. of results obtained in three independent experiments *$P<0.05$ and **$P<0.01$, versus corresponding values measured in untreated neurons; §§$P<0.01$, versus the corresponding value measured in WT neurons (ANOVA followed by the Student–Newman–Keul test).

of kinases known to be activated upon IGF-1R stimulation. Treating neurons with the Src family kinase inhibitor PP2, but not with its inactive analogue PP3 (10 µM each), entirely suppressed the induction of cAMP production by IGF-1 (Figure 4C). The IGF-1-mediated cAMP production was similarly inhibited by SU6656 (1 µM), a more selective inhibitor of this tyrosine kinase subfamily (Blake *et al*, 2000). Further supporting a role of Src family kinases in PAC1R transactivation, IGF-1 increased Src activity (assessed by phosphorylation of Tyr^{416} in the activation loop of the kinase domain; Figure 4B) and induced PAC1R phosphorylation on tyrosine residues in cortical neurons, an effect that was prevented by SU6656 (Figure 4A). In contrast, the increase in cAMP production in IGF-1-treated neurons was not prevented by wortmannin (100 nM), a PI3K inhibitor, by PD98056 (10 µM), an inhibitor of the Erk1,2 signalling pathway, or by the PKC inhibitor GF109203X (10 µM; Figure 4B). Together, these

findings suggest that PAC1R transactivation in IGF-1-treated neurons may result from PAC1R phosphorylation by a Src family kinase within a protein complex formed by PAC1 and IGF-1 receptors.

Role of PAC1 receptor transactivation in IGF-1 antiapoptotic activity

The ability of IGF-1 to promote neuronal survival has been attributed in part to the PI3-K/Akt pathway (Datta *et al*, 1997). As we have shown that PAC1R transactivation was involved in the phosphorylation and activation of Akt upon IGF-1 treatment, we addressed the possibility that PAC1R transactivation could also contribute to the reported neuroprotective activity of IGF-1 in cerebellar granule neurons (CGNs) (D'Mello *et al*, 1993; Galli *et al*, 1995). These neurons survive *in vitro* in the presence of depolarizing concentrations of KCl (25–30 mM) when they are serum-starved from
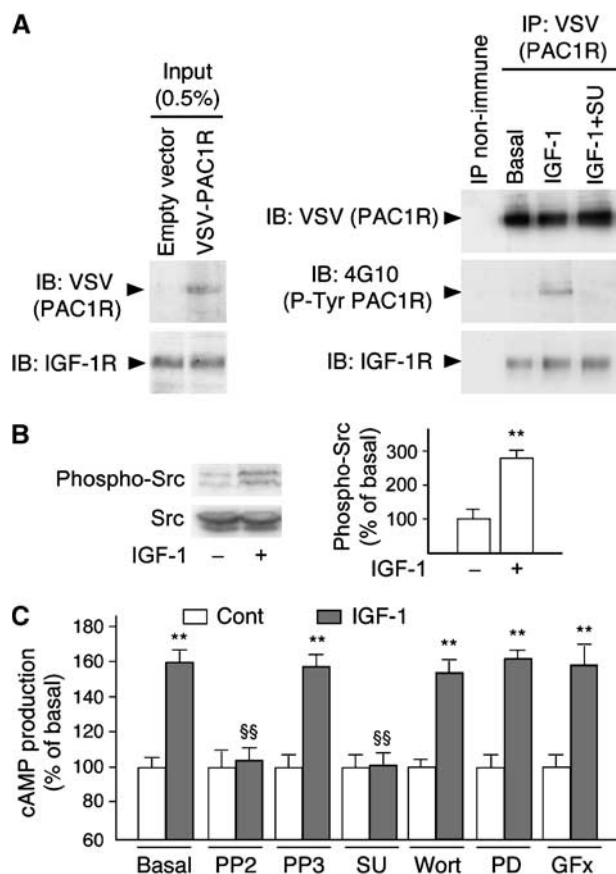
Figure 4 Role of Src family kinase in IGF-1-mediated transactivation of PAC1 receptors constitutively associated with IGF-1 receptors in cortical neurons. (**A**) Cortical neurons transfected with the indicated constructs were exposed for 10 min with 2.5 ng/ml IGF-1 in the absence or presence of 1 μM SU6656. Solubilized protein extracts were immunoprecipitated with a polyclonal anti-VSV antibody. Immunoprecipitated proteins were analyzed by immunoblotting using monoclonal antibodies against VSV or phosphotyrosines or the polyclonal IGF-1R antibody. (**B**) The phosphorylation of Src was analyzed by sequential immunoblotting with antibodies against phospho-Tyr[416] and total Src. Quantification of Src phosphorylation was performed by densitometric analysis using the NIH Image software. Data are means $\pm$ s.e.m. of results obtained in three independent experiments. **$P<0.01$, versus corresponding values measured in untreated neurons. (**C**) Neurons were exposed for 10 min in the absence or presence of IGF-1 and kinase inhibitors (also applied for 30 min before the IGF-1 challenge): PP2 (10 μM), PP3 (10 μM), SU6656 (SU, 1 μM), wortmannin (Wort, 100 nM), PD98056 (PD, 10 μM) and GF109203X (GFx, 10 μM). Results, expressed in % of basal cAMP level, are means $\pm$ s.e.m. of values obtained in five independent experiments. **$P<0.01$, versus corresponding values measured in the absence of IGF-1; $^{\S\S}P<0.01$, versus IGF-1-induced cAMP production measured in the absence of inhibitor (ANOVA followed by the Student–Newman–Keul test).

serum, whereas they undergo apoptosis in the presence of physiological KCl concentration (5 mM) (D'Mello et al, 1993). This apoptotic process is known to be prevented by IGF-1 or treatments that elevate intracellular cAMP levels (D'Mello et al, 1993; Galli et al, 1995). We found in cultured CGNs from PAC1$^{-/-}$ mice switched to 5 mM KCl that the ability of IGF-1 to prevent apoptosis was markedly reduced compared to cultures from WT mice (6 ± 1% of apoptotic cells in WT cultures treated with IGF-1 versus 32 ± 7% in their PAC1$^{-/-}$ counterparts, $n=3$, assessed by nuclear DNA staining with Hoechst 33258; Figure 5A and C). The reduced ability

of IGF-1 to support survival of PAC1$^{-/-}$ CGNs resulted from the loss of PAC1R expression rather than from a downregulation of some signalling molecules preventing apoptosis, as IGF-1 antiapoptotic activity was restored in PAC1$^{-/-}$ CGNs transfected with the VSV-PAC1R (Figure 5B and C). PACAP6-38 did not reduce the ability of IGF-1 to support survival of WT CGNs (Figure 5C). Collectively, these results indicate that transactivation of unliganded PAC1R plays an essential role in the antiapoptotic activity of IGF-1. Moreover, AG1478 did not inhibit the antiapoptotic action of IGF-1 (Figure 5C), consistent with the minor contribution of EGFR transactivation in the IGF-1R-associated phosphoproteome. Finally, we demonstrated that treating CGNs with IGF-1 increased the phosphorylation of Akt at Ser[473] during the timeframe of apoptosis induction (8 h; Figure 5D). As described above in cortical neurons, IGF-1-mediated Akt phosphorylation was strongly reduced in CGNs from PAC1$^{-/-}$ mice, further supporting the involvement of PAC1R transactivation in the recruitment by IGF-1 of the antiapoptotic PI3-K/Akt signalling pathway in CGNs.

In conclusion, our results demonstrate that a procedure based on the enrichment of PMAC followed by the purification of phosphopeptides by TiO$_2$ adsorption is an efficient method to decipher phosphoproteome changes induced by specific signalling pathways from a limited amount of neurons ($\sim$10 millions neurons). This procedure revealed a novel unexpected mechanism by which highjacking of the unliganded Gs-protein-coupled PAC1R is involved in IGF-1-mediated phosphorylation events and neuroprotective activity in neuronal cells. The present findings together with the recent demonstration of transactivation of unliganded CXCR4 receptors by IGF-1Rs (Akekawatchai et al, 2005) indicate that such a functional interaction with IGF-1R may be a function shared by several GPCRs. Whether IGF-1 and PAC1 receptors form dimers or they indirectly interact via additional protein partners remains to be established. It is likely that constitutive association of both receptors within a unique protein complex optimizes PAC1R transactivation by Src family kinases upon IGF-1 treatment.

Genetic inactivation of the genes encoding PACAP or PAC1R in mice generates complex CNS phenotypic changes including psychomotor abnormalities, altered synaptic plasticity and memory performance and dysfunctions of circadian rhythms (Hashimoto et al, 2006). These phenotypes may result from both developmental defects and alteration of PAC1R-mediated signalling. Whether the loss of IGF-1-mediated PAC1R transactivation contributes to these behavioral abnormalities requires further investigation. In any case, the complex signalling network associated with IGF-1Rs described herein may account for the unique properties of this growth factor to promote neuronal polarity (Sosa et al, 2006) and the survival of numerous neuronal populations (Russo et al, 2005), compared with other neurotrophins.

Materials and methods

Animals, plasmids and reagents

C57BL/6J mice were obtained from Charles Rivers. The PAC1R-deficient mice were described previously (Jamen et al, 2000).

Using PCR, the mouse PAC1R (IMAGE 6852762) was N-terminally tagged with the sequence encoding an 11-amino-acid epitope (YTDIEMNRLGK) of the VSV glycoprotein. The amplified
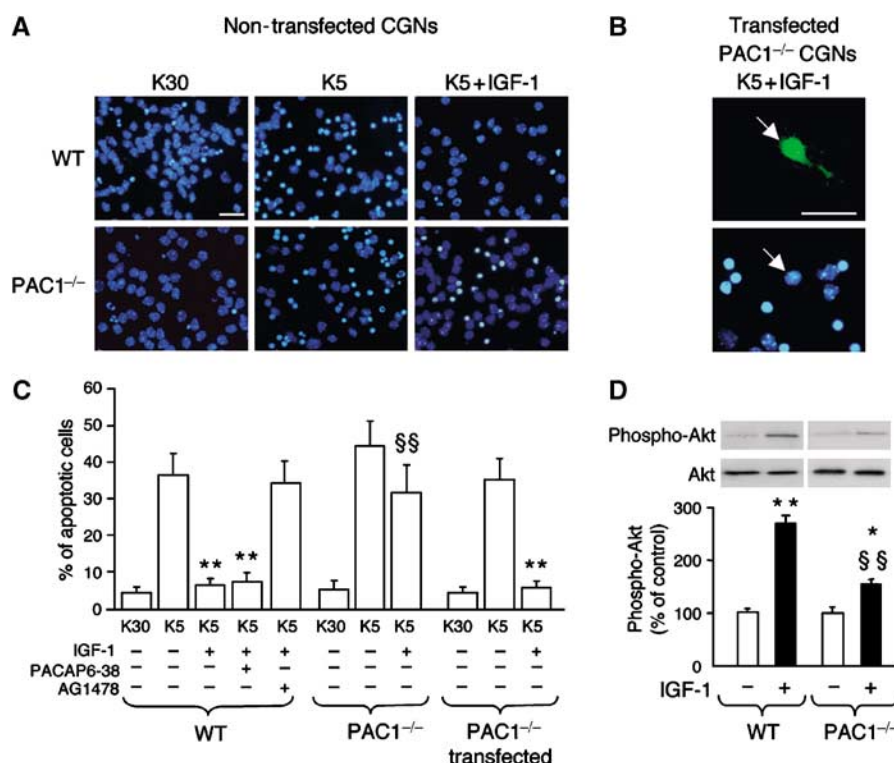
Figure 5 Role of PAC1 receptor transactivation in the antiapoptotic activity of IGF-1 in CGNs. (**A**) CGNs from WT and PAC1$^{-/-}$ mice, grown for 7 days in a culture medium containing 30 mM KCl + 10% fetal calf serum were switched for 8 h to a serum-free medium containing either 30 mM KCl (K30), 5 mM KCl (K5) or K5 + IGF-1 (2.5 ng/ml). (**B**) Cultured CGNs from PAC1$^{-/-}$ mice, transfected with the pCI/VSV-PAC1R construct, were switched for 8 h to a serum-free medium containing K5 + IGF-1. Transfected neurons (arrows) were detected by VSV immunolabelling. Nuclei were stained with Hoechst 33258. Fluorescence photomicrographs of representative fields are illustrated. Dense or fragmented nuclei were considered as apoptotic. Scale bars, 20 μm. (**C**) The quantification of apoptotic nuclei is shown. Data, expressed as percentage of apoptotic cells, are the means ± s.e.m. of results obtained in three independent experiments. **$P < 0.01$, versus K5; §§$P < 0.01$, versus the corresponding value measured in WT neurons (ANOVA followed by the Student–Newman–Keul test). (**D**) PAC1R transactivation is involved in the phosphorylation of Akt induced by IGF-1 in CGNs. CGNs from WT and PAC1$^{-/-}$ mice were switched for 8 h to a serum-free medium containing either K5 or K5 + IGF-1. Akt phosphorylation was analyzed by sequential immunoblotting with antibodies against phospho-Ser^{473}Akt and total Akt. Quantification of Akt phosphorylation level was performed by densitometric analysis. Data are means ± s.e.m. of values obtained in three independent experiments. *$P < 0.05$ and **$P < 0.01$, versus corresponding values measured in untreated neurons; §§$P < 0.01$, versus the corresponding value measured in WT neurons.

DNA was directly subcloned into the *Nhe*I and *Eco*RI restriction sites of pCI vector, yielding the pCI/VSV-mPAC1 construct.

The rabbit polyclonal antibodies against phospho-Tyr^{845} EGFR, phospho-Tyr^{1068} EGFR, EGFR, phospho-Tyr$^{1135/1136}$ IGF-1R, IGF-1R, phospho-Ser/Thr PKA substrates, phospho-Thr^{202}/Tyr^{204} Erk1,2, total Erk1,2, phospho-Ser^{473} Akt and total Akt, phospho-Tyr^{416} Src and total Src were purchased from Cell Signalling Technology and the mouse monoclonal antibody against phosphotyrosine (clone 4G10) from Upstate Biotechnology. PACAP38 and PACAP6-38 were obtained from Neosystem, AG1478 and U73122 from Calbiochem and SU6656 from Sugen. All other reagents were from Sigma. Phosphoprotein enrichment kits were purchased from Clontech. TiO$_2$ beads were obtained from a disassembled TiO$_2$ cartridge (4.0 mm inner diameter, catalogue number 5020–08520-5u-TiO$_2$), purchased from GL Sciences Inc. ^{32}P-orthophosphoric acid (5 mCi/mmol) was obtained from GE Healthcare.

Primary neuronal cultures and transfection

Primary cultures of cortical neurons were prepared using the method of el-Etr *et al* (1989). Briefly, cortices were removed from 17-day-old WT or PAC1$^{-/-}$ mouse embryos and mechanically dissociated in PBS containing 33 mM glucose. Cells were seeded on either 100-mm culture dishes (12 × 10^6 cells/dish), six-well plates (2 × 10^6 cells/well) or 24-well plates (5 × 10^5 cells/well), and maintained for 7 days at 37°C in a humidified atmosphere containing 95% CO$_2$ in a serum-free culture medium including a 1:1 mixture of Dulbecco's modified Eagle's medium and F12 nutrient supplemented with D-glucose (33 mM), L-glutamine (2 mM), NaHCO$_3$ (13 mM), HEPES buffer (5 mM, pH 7.4), penicillin–streptomycin (100 IU/ml

and 100 μg/ml, respectively) and a mixture of salt and hormones containing insulin (25 μg/ml), transferrin (100 μg/ml), progesterone (20 nM), putrescine (60 mM) and Na$_2$SeO$_3$ (30 nM). Under these conditions, cultures were shown to be highly enriched in neurons by immunocytochemistry using a mouse anti-MAP2 antibody (clone AP20, Sigma) and devoid of glial cells, as assessed by the absence of immunolabelling using a rabbit antibody against glial fibrillary acid protein (Dako, not shown).

Primary cultures of CGNs were prepared from 7-day-old WT or PAC1$^{-/-}$ mice as described previously (Van Vliet *et al*, 1989). Freshly dissected cerebella were incubated with 0.25 mg/ml trypsin for 10 min at 37°C. Trypsin inhibitor (0.5 mg/ml) and DNAase 1 (0.08 mg/ml) were added and cerebella were mechanically dissociated. Cells were seeded on 15-mm glass coverslips (3 × 10^5 cells/coverslip) and grown for 7 days in culture medium composed of basal Eagle's medium, supplemented with KCl (30 mM final), glutamine (2 mM), HEPES buffer (5 mM, pH 7.4), penicillin–streptomycin (100 IU/ml and 100 μg/ml, respectively) and 10% fetal calf serum. Cytosine arabinoside (30 μM) was added 24 h after plating to prevent proliferation of non-neuronal cells.

Cultures were transfected 6 days after seeding with the pCI/VSV-PAC1 plasmid (1 μg DNA/10^6 cells) by using Lipofectamine 2000, according to the manufacturer's instructions. Experiments were carried out 24 h after transfection.

Phosphoprotein enrichment

Neuronal protein extracts were enriched in phosphoproteins using the PMAC kit. Neurons, grown in 100-mm culture dishes for 7 days ($\sim$10^7 cells/dish) were incubated for 3 h in HEPES saline buffer

(containing (in mM) HEPES, 20, pH 7.4; NaCl, 150; KCl, 4.2; CaCl₂, 0.9; MgCl₂ 0.5 and glucose, 10), and then exposed to indicated treatments for 10 min in HEPES saline buffer. Cells were scraped off, spun at $1000\,g$, washed three times in PBS containing 33 mM glucose and frozen at -80°C. The cells were lysed, and cell lysates (4 mg protein) were loaded onto PMAC columns according to the manufacturer's instructions. Proteins retained by the column were eluted with 3 ml of phosphate buffer (NaCl, 0.5 M; sodium-phosphate, 20 mM, pH 7.2). Eluted proteins were precipitated with 10% trichloroacetic acid for 2 h at 4°C. Samples were centrifuged at $10\,000\,g$ for 30 min and pellets were washed three times with diethyl ether.

Two-dimensional gel electrophoresis

Protein pellets were resuspended in 350 μl of isoelectrofocusing medium containing urea (7 M), thiourea (2 M), CHAPS (4%), ampholines (preblended, pI 3.5–9.5, 8 mg/ml; GE Healthcare), dithiothreitol (100 mM), tergitol NP7 (0.2%, Sigma) and traces of bromophenol blue. Proteins were then resolved onto 2D gels and stained with silver, as described previously (Delcourt et al, 2005). Gels to be compared were always processed and stained in parallel. Gels were scanned using a computer-assisted densitometer. ³²P-labelled proteins were detected by autoradiography (3-day exposure).

MALDI-TOF-MS and protein identification

Protein spots were excised and in-gel digested using trypsin (Gold, Promega), as described previously (Delcourt et al, 2005). Digested samples were dehydrated in a vacuum centrifuge, solubilized in 10 μl of formic acid (2%), desalted using C18 ZipTips (Millipore, elution with 10 μl of 0.1% TFA–50% acetonitrile) and concentrated to a 1 μl volume. A total of 0.3 μl, mixed with the same volume of α-cyano-4-hydroxy-trans-cinnamic acid (10 mg/ml in 0.1% TFA in 50% acetonitrile), was deposited on a 384-well MALDI target using the dry droplet procedure and air-dried at room temperature. Analyses were performed using an UltraFlex MALDI-TOF/TOF mass spectrometer (Bruker-Franzen Analytik) operating in the reflectron mode with a 20 kV accelerating voltage and a 70-ns delayed extraction. Mass spectra were acquired in the automatic mode using the AutoXecute™ module of Flexcontrol™ (laser power ranged from 30 to 70%, 500 shots). Spectra were analyzed using FlexAnalysis™ software (Bruker–Franzen Analytik) and auto-proteolysis peptides of trypsin (m/z 842.51, 1045.56 and 2211.10) were used as internal calibrates. Peptides were selected in the mass range of 900–4000 Da. Proteins were identified using the Mascot software package (version 2.1, Matrixscience) against the Swiss-Prot database. The following parameters were used for database interrogation: mass tolerance of 50 p.p.m. (even if the mass accuracy of our analyses was usually better than 20 p.p.m.); fixed chemical modification: carbamidomethylation of cysteines; variable chemical modification, oxidation of methionines; matching peptides with one missed cleavage accepted only when they included two consecutive basic residues or when arginine or lysine residues were followed by one or several acidic residues inside the peptide amino-acid sequence. Mascot scores higher than 53 were considered as significant ($P<0.05$) for Swiss-Prot database interrogation.

MS/MS spectra were acquired on the UltraFlex MALDI-TOF/TOF mass spectrometer employing the LIFT™ technology. This mode enables the production of ions from laser-induced metastable decay. A relatively low voltage of 8 kV was initially applied for ion acceleration. The parent ion mass selector window was in the range of 0.5–1%. Fragments generated from laser-induced dissociation were subsequently increased to a higher potential (19 kV) in the LIFT cell. Automatic calibration was performed using the Flexcontrol™ software for the parent ion and the FlexAnalysis™ software for the entire spectrum. A mass deviation of 0.5 Da was allowed for database interrogation for fragment ions. Database interrogation was performed using the Mascot software against the Swiss-Prot database, with phospho-Ser/Thr/Tyr as variable modification. Mascot scores higher than 25 were considered as significant ($P<0.05$) for Swiss-Prot database interrogation.

Purification of phosphorylated peptides on TiO₂ microcolumns

TiO₂ microcolumns (3 mm length) were packed in GELoader tips as described by Larsen et al (2005). Lyophilized samples digested with

trypsin were solubilized in 10 μl of 80% acetonitrile, 0.1% TFA, 200 mg/ml dihydroxybutyric acid (DHB) and loaded onto the microcolumns. The columns were washed with 10 μl of the DHB solution and 10 μl of 80% acetonitrile, and 0.1% TFA. Peptides retained by the column were eluted with 5 μl NH₄OH (pH 10.5).

[¹²⁵I]PACAP-binding assay

Mice brains were gently homogenized in 10 volumes of ice-cold binding buffer containing Tris–HCl (50 mM, pH 7.4), MgCl₂ (5 mM) and a protease inhibitor cocktail using a glass-Teflon homogenizer. The homogenates were centrifuged at $1000\,g$ for 10 min at 4°C, and the resulting supernatant was centrifuged at $50\,000\,g$ for 30 min at 4°C. The final pellet was gently resuspended in binding buffer. Competitive binding was performed by incubating 20 μg of membrane proteins with 50 pM [¹²⁵I]PACAP27 (2200 Ci/mmol; Perkin–Elmer) and increasing amounts of cold PACAP27 for 60 min at 25°C. Nonspecific binding was determined in the presence of 10 nM PACAP 6-38. Binding data were calculated from three independent experiments performed in triplicate. Binding data analysis was carried out using the Prism 4 software (GraphPad Software Inc.).

Co-immunoprecipitation

Cortical neurons transfected with the pCI/VSV-PAC1R construct (2×10^{7} neurons per assay) were lysed in solubilization buffer containing HEPES, 50 mM, pH 7.5; EDTA, 1 mM; Triton X-100, 1%; SDS, 0.1%; Na₃VO₄, 1 mM; sodium-pyrophosphate, 30 mM; NaF, 10 mM and a protease inhibitor cocktail. Solubilized proteins were incubated overnight at 4°C with 5 μl of rabbit non-immune serum or the polyclonal anti-VSV antibody. Samples were then incubated for 1 h with 50 μl protein of protein A Sepharose beads. After five washes in PBS, immunoprecipitated proteins were eluted in SDS sample buffer.

Immunoblotting

Proteins were resolved on 12.5% gels and transferred electrophor-etically onto nitrocellulose membranes (Hybond-C, GE Healthcare). Membranes were incubated in blocking buffer (Tris–HCl, 50 mM, pH 7.5; NaCl, 200 mM; Tween 20, 0.1% and skimmed dry milk, 5%) for 1 h at room temperature and incubated overnight with primary antibodies, all at 1:1000 dilution, in blocking buffer. Blots were washed three times with blocking buffer and incubated with either horseradish peroxidase-conjugated anti-rabbit or anti-mouse antibodies (GE Healthcare, 1:3000 in blocking buffer) for 1 h at room temperature. Immunoreactivity was detected with an enhanced chemiluminescence method (Renaissance Plus, Perkin–Elmer).

Measurement of cAMP production

Neurons grown in 24-well culture dishes were pre-incubated with HEPES saline buffer for 3 h and then exposed for 5 or 10 min to the indicated treatments in 0.25 ml HEPES saline buffer supplemented with 0.1% BSA and 3-isobutyl-1-methyl xanthine (IBMX, 1 mM), a nonspecific phoshodiesterase inhibitor. Cells were then lysed by adding 0.25 ml Triton X-100 (0.1%). Intracellular cAMP levels were measured using a homogenous time-resolved fluorescence-based cAMP dynamic kit (CisBio International) according to the manufacturer's instructions.

Induction of apoptosis, immunocytochemistry and measurement of apoptotic nuclei

CGNs grown for 7 days on glass coverslips were washed three times with a serum-free medium composed of basal Eagle's medium supplemented with glucose (30 mM), glutamine (2 mM), HEPES buffer (5 mM, pH 7.4) and penicillin–streptomycin (100 IU/ml and 100 μg/ml, respectively), and incubated for 8 h in this medium in the presence of the indicated treatments. Cells were then exposed to propidium iodide (3 μg/ml) for 10 min, to assess possible lack of membrane integrity associated with cell necrosis. CGNs were then washed twice with PBS containing 33 mM glucose, fixed with 4% paraformaldehyde in PBS (30 min at 4°C) and incubated with Hoechst 33258 (1 μg/ml for 10 min at room temperature). VSV-PAC1-transfected CGNs were detected by immunolabelling with a monoclonal anti-VSV antibody (1:1000 dilution) and an alexa green-labelled anti-mouse antibody (1:2000 dilution). Nuclear DNA staining and VSV immunoreactivity were examined by digital fluorescence imaging microscopy (Axiophot 2 microscope, Zeiss).

Condensed and/or fragmented nuclei were considered as apoptotic. Data, expressed in % of apoptotic cells, are the mean±s.e.m. of values obtained in three independent experiments (⩾450 cells originating from three coverslips counted per experiment).

Supplementary data

Supplementary data are available at *The EMBO Journal* Online (http://www.embojournal.org).

References

Aigner L, Arber S, Kapfhammer JP, Laux T, Schneider C, Botteri F, Brenner HR, Caroni P (1995) Overexpression of the neural growth-associated protein GAP-43 induces nerve sprouting in the adult nervous system of transgenic mice. *Cell* **83:** 269–278

Akekawatchai C, Holland JD, Kochetkova M, Wallace JC, McColl SR (2005) Transactivation of CXCR4 by the insulin-like growth factor-1 receptor (IGF-1R) in human MDA-MB-231 breast cancer epithelial cells. *J Biol Chem* **280:** 39701–39708

Arimura A, Somogyvari-Vigh A, Weill C, Fiore RC, Tatsuno I, Bay V, Brenneman DE (1994) PACAP functions as a neurotrophic factor. *Ann NY Acad Sci* **739:** 228–243

Bai J, Ramos RL, Ackman JB, Thomas AM, Lee RV, LoTurco JJ (2003) RNAi reveals doublecortin is required for radial migration in rat neocortex. *Nat Neurosci* **6:** 1277–1283

Bertelsen LS, Barrett KE, Keely SJ (2004) Gs protein-coupled receptor agonists induce transactivation of the epidermal growth factor receptor in T84 cells: implications for epithelial secretory responses. *J Biol Chem* **279:** 6271–6279

Blake RA, Broome MA, Liu X, Wu J, Gishizky M, Sun L, Courtneidge SA (2000) SU6656, a selective src family kinase inhibitor, used to probe growth factor signaling. *Mol Cell Biol* **20:** 9018–9027

Carey RG, Li B, DiCicco-Bloom E (2002) Pituitary adenylate cyclase activating polypeptide anti-mitogenic signaling in cerebral cortical progenitors is regulated by p57Kip2-dependent CDK2 activity. *J Neurosci* **22:** 1583–1591

Collins MO, Yu L, Coba MP, Husi H, Campuzano I, Blackstock WP, Choudhary JS, Grant SG (2005) Proteomic analysis of *in vivo* phosphorylated synaptic proteins. *J Biol Chem* **280:** 5972–5982

Copani A, Casabona G, Bruno V, Caruso A, Condorelli DF, Messina A, Di Giorgi Gerevini V, Pin JP, Kuhn R, Knopfel T, Nicoletti F (1998) The metabotropic glutamate receptor mGlu5 controls the onset of developmental apoptosis in cultured cerebellar neurons. *Eur J Neurosci* **10:** 2173–2184

D'Mello SR, Galli C, Ciotti T, Calissano P (1993) Induction of apoptosis in cerebellar granule neurons by low potassium: inhibition of death by insulin-like growth factor I and cAMP. *Proc Natl Acad Sci USA* **90:** 10989–10993

Datta SR, Dudek H, Tao X, Masters S, Fu H, Gotoh Y, Greenberg ME (1997) Akt phosphorylation of BAD couples survival signals to the cell-intrinsic death machinery. *Cell* **91:** 231–241

Datta SR, Katsov A, Hu L, Petros A, Fesik SW, Yaffe MB, Greenberg ME (2000) 14-3-3 proteins and survival kinases cooperate to inactivate BAD by BH3 domain phosphorylation. *Mol Cell* **6:** 41–51

Delcourt N, Jouin P, Poncet J, Demey E, Mauger E, Bockaert J, Marin P, Galeotti N (2005) Difference in mass analysis using labeled lysines (DIMAL-K): a new, efficient proteomic quantification method applied to the analysis of astrocytic secretomes. *Mol Cell Proteomics* **4:** 1085–1094

Dudek H, Datta SR, Franke TF, Birnbaum MJ, Yao R, Cooper GM, Segal RA, Kaplan DR, Greenberg ME (1997) Regulation of neuronal survival by the serine-threonine protein kinase Akt. *Science* **275:** 661–665

el-Etr M, Cordier J, Glowinski J, Premont J (1989) A neuroglial cooperativity is required for the potentiation by 2-chloroadenosine of the muscarinic-sensitive phospholipase C in the striatum. *J Neurosci* **9:** 1473–1480

El-Shewy HM, Johnson KR, Lee MH, Jaffa AA, Obeid LM, Luttrell LM (2006) Insulin-like growth factors mediate heterotrimeric G protein-dependent ERK1/2 activation by trans-activating sphingosine 1-phosphate receptors. *J Biol Chem* **281:** 31399–31407

Fan Z, Beresford PJ, Oh DY, Zhang D, Lieberman J (2003) Tumor suppressor NM23-H1 is a granzyme A-activated DNase during CTL-mediated apoptosis, and the nucleosome assembly protein SET is its inhibitor. *Cell* **112:** 659–672

Galli C, Meucci O, Scorziello A, Werge TM, Calissano P, Schettini G (1995) Apoptosis in cerebellar granule cells is blocked by high KCl, forskolin, and IGF-1 through distinct mechanisms of action: the involvement of intracellular calcium and RNA synthesis. *J Neurosci* **15:** 1172–1179

Guirland C, Buck KB, Gibney JA, DiCicco-Bloom E, Zheng JQ (2003) Direct cAMP signaling through G-protein-coupled receptors mediates growth cone attraction induced by pituitary adenylate cyclase-activating polypeptide. *J Neurosci* **23:** 2274–2283

Hashimoto H, Shintani N, Baba A (2006) New insights into the central PACAPergic system from the phenotypes in PACAP- and PACAP receptor-knockout mice. *Ann NY Acad Sci* **1070:** 75–89

Hayashi K, Shirao T (1999) Change in the shape of dendritic spines caused by overexpression of drebrin in cultured cortical neurons. *J Neurosci* **19:** 3918–3925

Jamen F, Persson K, Bertrand G, Rodriguez-Henche N, Puech R, Bockaert J, Ahren B, Brabet P (2000) PAC1 receptor-deficient mice display impaired insulinotropic response to glucose and reduced glucose tolerance. *J Clin Invest* **105:** 1307–1315

Kaspar BK, Llado J, Sherkat N, Rothstein JD, Gage FH (2003) Retrograde viral delivery of IGF-1 prolongs survival in a mouse ALS model. *Science* **301:** 839–842

Lapucci A, Donnini M, Papucci L, Witort E, Tempestini A, Bevilacqua A, Nicolin A, Brewer G, Schiavone N, Capaccioli S (2002) AUF1 is a bcl-2 A+U-rich element-binding protein involved in bcl-2 mRNA destabilization during apoptosis. *J Biol Chem* **277:** 16139–16146

Larsen MR, Thingholm TE, Jensen ON, Roepstorff P, Jorgensen TJ (2005) Highly selective enrichment of phosphorylated peptides from peptide mixtures using titanium dioxide microcolumns. *Mol Cell Proteomics* **4:** 873–886

Lee FS, Rajagopal R, Kim AH, Chang PC, Chao MV (2002) Activation of Trk neurotrophin receptor signaling by pituitary adenylate cyclase-activating polypeptides. *J Biol Chem* **277:** 9096–9102

Leinninger GM, Backus C, Uhler MD, Lentz SI, Feldman EL (2004) Phosphatidylinositol 3-kinase and Akt effectors mediate insulin-like growth factor-I neuroprotection in dorsal root ganglia neurons. *FASEB J* **18:** 1544–1546

Marin P, Nastiuk KL, Daniel N, Girault JA, Czernik AJ, Glowinski J, Nairn AC, Premont J (1997) Glutamate-dependent phosphorylation of elongation factor-2 and inhibition of protein synthesis in neurons. *J Neurosci* **17:** 3445–3454

Morio H, Tatsuno I, Hirai A, Tamura Y, Saito Y (1996) Pituitary adenylate cyclase-activating polypeptide protects rat-cultured cortical neurons from glutamate-induced cytotoxicity. *Brain Res* **741:** 82–88

Rajagopal R, Chen ZY, Lee FS, Chao MV (2004) Transactivation of Trk neurotrophin receptors by G-protein-coupled receptor ligands occurs on intracellular membranes. *J Neurosci* **24:** 6650–6658

Russo VC, Gluckman PD, Feldman EL, Werther GA (2005) The insulin-like growth factor system and its pleiotropic functions in brain. *Endocr Rev* **26:** 916–943

Sosa L, Dupraz S, Laurino L, Bollati F, Bisbal M, Caceres A, Pfenninger KH, Quiroga S (2006) IGF-1 receptor is essential for the establishment of hippocampal neuronal polarity. *Nat Neurosci* **9:** 993–995

Stessin AM, Zippin JH, Kamenetsky M, Hess KC, Buck J, Levin LR (2006) Soluble adenylyl cyclase mediates nerve growth factor-induced activation of Rap1. *J Biol Chem* **281:** 17253–17258

Subramaniam S, Shahani N, Strelau J, Laliberte C, Brandt R, Kaplan D, Unsicker K (2005) Insulin-like growth factor 1 inhibits extracellular signal-regulated kinase to promote neuronal survival via the phosphatidylinositol 3-kinase/protein kinase A/c-Raf pathway. *J Neurosci* **25:** 2838–2852

Suh J, Lu N, Nicot A, Tatsuno I, DiCicco-Bloom E (2001) PACAP is an anti-mitogenic signal in developing cerebral cortex. *Nat Neurosci* **4:** 123–124

Takei N, Skoglosa Y, Lindholm D (1998) Neurotrophic and neuroprotective effects of pituitary adenylate cyclase-activating polypeptide (PACAP) on mesencephalic dopaminergic neurons. *J Neurosci Res* **54:** 698–706

Takei N, Torres E, Yuhara A, Jongsma H, Otto C, Korhonen L, Abiru Y, Skoglosa Y, Schutz G, Hatanaka H, Sofroniew MV, Lindholm D (2000) Pituitary adenylate cyclase-activating polypeptide promotes the survival of basal forebrain cholinergic neurons *in vitro* and *in vivo*: comparison with effects of nerve growth factor. *Eur J Neurosci* **12:** 2273–2280

Tanaka T, Serneo FF, Tseng HC, Kulkarni AB, Tsai LH, Gleeson JG (2004) Cdk5 phosphorylation of doublecortin ser297 regulates its effect on neuronal migration. *Neuron* **41:** 215–227

Van Vliet BJ, Sebben M, Dumuis A, Gabrion J, Bockaert J, Pin JP (1989) Endogenous amino acid release from cultured cerebellar neuronal cells: effect of tetanus toxin on glutamate release. *J Neurochem* **52:** 1229–1239

Vaudry D, Gonzalez BJ, Basille M, Fournier A, Vaudry H (1999) Neurotrophic activity of pituitary adenylate cyclase-activating polypeptide on rat cerebellar cortex during development. *Proc Natl Acad Sci USA* **96:** 9415–9420

Villalba M, Bockaert J, Journot L (1997) Pituitary adenylate cyclase-activating polypeptide (PACAP-38) protects cerebellar granule neurons from apoptosis by activating the mitogen-activated protein kinase (MAP kinase) pathway. *J Neurosci* **17:** 83–90

Vincent AM, Mobley BC, Hiller A, Feldman EL (2004) IGF-I prevents glutamate-induced motor neuron programmed cell death. *Neurobiol Dis* **16:** 407–416